GEOMETRIC EVALUATION USING CONSTRUCTAL DESIGN OF A COASTAL OVERTOPPING DEVICE WITH DOUBLE RAMP CONSIDERING A REGULAR WAVE AND TIDAL VARIATION

J. C. Martins[a],
M. M. Goulart[b],
E. D. dos Santos[b],
L. A. Isoldi[b],
M. N. Gomes[c],
and L. A. O. Rocha[d]

[a]Universidade Federal do Rio Grande do Sul
Escola de Engenharia
Rua Sarmento Leite, 425, CEP 90050-170
Porto Alegre, Rio Grande do Sul, Brasil
jaifercm@gmail.com
[b]Universidade Federal do Rio Grande
Escola de Engenharia
Av. Itália, km 8, CP 474, CEP 96201-900
Rio Grande, Rio Grande do Sul, Brasil
moraesgoulart@yahoo.com.br
elizaldosantos@furg.br
liercioisoldi@furg.br
[c]Instituto Federal do Paraná
Rua Antonio Carlos Rodrigues, 453
CEP 83215-750, Paranaguá, Paraná, Brasil
mateus.gomes@ifpr.edu.br
[d]Universidade do Vale do Rio dos Sinos
Av. Unisinos, 950, CEP 93022-750
São Leopoldo, Rio Grande do Sul, Brasil
laorocha@gmail.com

ABSTRACT

Concern for the environment and new ways of electricity generation, have led to studies of renewable energy sources, among these the Wave Energy Converters (WECs) are an option, however there are still many challenges to define how best to realize the conversion of the energy of the waves into electricity. In this work, a numerical study was carried out with the purpose of maximizing the available power (P_d) of a two-ramp overtopping device, considering the area fraction of ramps (ϕ_1 and ϕ_2) equal to 0.0006 and the ratio between height and length of the ramps ($H_1/L_1 = H_2/L_2$) equal to 0.3. The distance between the ramps (L_g) was varied in three values: 1.0; 1.5 and 2.0 m, besides three values for the free surface of water (h): 9.8; 10.0 and 10.2 m; simulating a tidal effect. The Constructal Design and Exhaustive Search methods were used, respectively, in the geometric evaluation (determination of a search field) and optimization. For the wave generation, the Second Order Stokes Theory was used, with wave period (T) of 7.5 s and wave height (H) 1.0 m. The results showed that there was no accumulation of water in the upper ramp of the device, in addition, with the increase of L_g there was an increase of P_d in h = 10.0 and 10.2 m, and P_d kept practically constant in h = 9, 8 m. And, as expected, with increasing of h, there was an increase in P_d.

Keywords: renewable energy; waves of the sea; overtopping; tidal

Received: February 22, 2019
Revised: March 18, 2019
Accepted: April 19, 2019

NOMENCLATURE

$A_{r,i}$	ramp area, m^2
A_T	flume area, m^2
g	gravitational acceleration, m/s^2
h	water depth, m
H	wave height, m
$h_{a,i}$	water height inside reservoir, m
H_i	ramp height, m
$H_{R,i}$	reservoir height, m
H_s	significant wave height, m
H_i/L_i	ratio between height and length of the ramp
H_T/L_T	ratio between height and length of the flume
k	wave number, m^{-1}
L_g	length between ramps, m
$L_{R,i}$	reservoir length, m
P_d	available power, W/m
P_{abs}	atmospheric pressure, kPa
T	wave period, s
t_i	initial time, s
t_f	final time, s
x	horizontal direction
y	dimension perpendicular to the plane
z	vertical direction

Greek symbols

α	volume fraction
λ	wave length, m
μ	viscosity, Pa.s
ρ	density, kg/m^3

σ angular frequency, rad.s^{-1}
$\bar{\bar{\tau}}$ deformation tensor, N/m²
ϕ ramp area fraction

Subscripts

a water
d available
f final
g gap
i low tank (1); upper tank (2)
m maximized
r ramp
R reservoir
s significant
T tank
∞ infinity

INTRODUCTION

Several studies on new forms of electricity generation with less environmental impact have been conducted every year. Many are the factors that lead to the search for renewable alternatives, among them the increase of the world population. One alternative is the use of energy from ocean waves, an area with a few studies, but none of them consolidated. The sea has a great energy potential, for example, southern Brazil where it is estimated a potential of 30kW wave meter. (Cruz and Sarmento, 2004).

The literature shows a variety of possible equipment, among them stands out the overtopping device by the simplicity of the operating principle. It is an equipment with a ramp, on which sea water incident overtop, accumulating in a reservoir. Then the water flows through a low head turbine (generating electricity) returning to the sea (Fleming, 2012). An illustration is shown in Fig. 1.

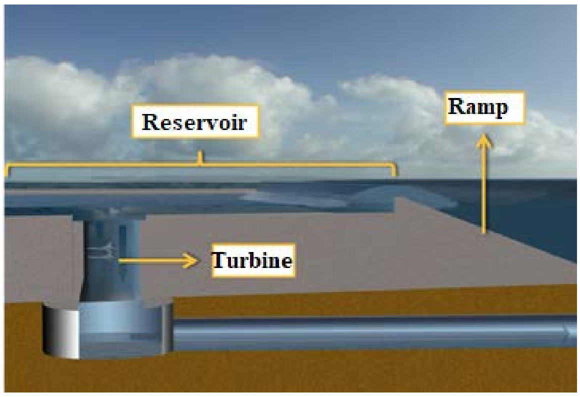

Figure 1. Illustration of the operation principle of the overtopping device. (Aqua-RET, 2012).

It is possible to find in the literature several studies on the overtopping device, for example, work on experimental evaluation of device parameters: Margheritini et al. (2009), Vicinanza et al. (2014), Liu et al. (2017) and Contestabile et al. (2017).

However, in relation to the numerical work, can cite: Margheritini et al. (2012), Nørgaard and Andersen (2012), Barbosa et al. (2017) and Jungrungruengtaworn and Hyun (2017).

Although, studies about the Constructal Design method in overtopping devices, there is an expressive amount of studies in the literature, among them: Goulart et al. (2015), Martins et al. (2015), Machado et al. (2017), Martins et al. (2017) and Martins et al. (2018).

Therefore, it is intended to evaluate geometrically the influence of the distance between ramps (L_g) of a double ramp overtopping device in real scale, and, the tide variation (h) over the available power (P_d). The Constructal Design method was used (Bejan, 2000; Bejan and Lorente, 2008) for determining a search field (based on restrictions and degrees of freedom) together with the Exhaustive Search method for optimization. Thus, three values were used for the distance between the ramps (L_g), 1.0 m, 1.5 m and 2.0 m; and three different depths (h) of the free surface of the water 9.8 m, 10.0 m and 10.2 m, representing the tide variation. To this, they were considered fixed ramps of the area fraction ($\phi_1 = \phi_2 = 0.0006$) and are ratios of heights and lengths of ramps ($H_1/L_1 = H_2/L_2 = 0.3$). In addition, the software Ansys Workbench® and Fluent® v.16 (Ansys, 2016) were used for pre-processing and processing, respectively, and Microsoft Excel® for post-processing. Already for the development of ocean waves, the Second Order Stokes Theory was used.

MATHEMATICAL MODELING

The physical domain studied is illustrated in Fig. 2. This is a two-dimensional (x in the horizontal and z in the vertical) two-ramp overtopping device placed on a real scale wave flume, where the third dimension (y) is perpendicular to the plane of the figure.

The (regular) wave is imposed at the input boundary of the domain in the zone defined as water (blue line - prescribed velocity) through two velocity components defined by the Second Order Stokes Theory (Chakrabarti, 2005). According to Almeida et al. (1997), the Rio Grande do Sul (RS) coast presents medium to high energy waves, with a significant height (H_s) of 1.5 m and a period (T) between 7.0 and 9.0 s. These characteristics are evaluated by Lisboa et al. (2016).

From this, the parameter of the regular wave chosen were: height (H) of 1 m, the period (T) equal to 7.5 s (hence, wavelength (λ) of 65.4 m to depth of 10 m). Another important parameter is the depth of the water depth (h), for which was used the average value out of 10 m, in addition, was considered a tidal variation of 0.20 m (up and down), yielding the values of h equals 9.8 and 10.2 m. For, the coast of RS is characterized by astronomical tides with a mean amplitude of 0.25 m (Almeida et al., 1997).

The flume has the following main dimensions: height (H_T) equal to 20 m (20*H) and length (L_T) of 327 m (5*λ), arriving to the ratio H_T/L_T of 0.0612.

The overtopping device has the following dimensions: lengths of the ramps L_1 and L_2; ramps heights H_1 and H_2; ramp areas $A_{r,1}$ and $A_{r,2}$; lengths and heights of the reservoirs, respectively, $L_{R,1}$ (equal to 20 m) and $L_{R,2}$ (equal to: 13,885, 13,385 and 12,885 m, due to the variation of L_g); $H_{R,1}$ and $H_{R,2}$, besides the heights $h_{a,1}$ and $h_{a,2}$ which represent the height of water accumulated in the reservoirs.

For the distance between the ramps (L_g) are three values used 1.0 m; 1.5 m and 2.0 m. The ramp area fractions (ϕ_1 and ϕ_2) were considered equal to 0.0006, and the ratio between the height and length of the ramps (slope) H_1/L_1 and H_2/L_2 the value used was 0.3 (~16.7°). Note that the crowning of the lower ramp was maintained at 10.6 m fix the wave relative to the channel bottom.

The objective of this study is to evaluate the influence of distance L_g (1.0 m, 1.5 m and 2.0 m) and tidal variation (0.20 m in relation of h = 10 m) on the available power (P_d).

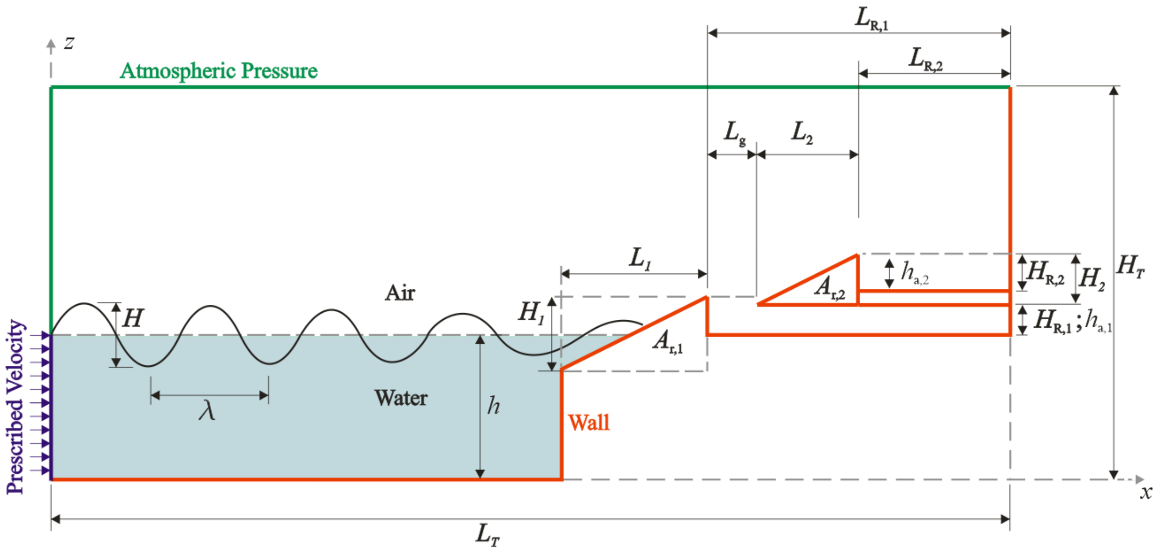

Figure 2. Computational domain of the analysis device analyzed.

Constructal Design Applied to the Overtopping Device

The Constructal Design is used in the geometric evaluation together with the Exhaustive Search optimization method in order to identify the best geometries in relation to the physical conditions employed during the study. In this work two restrictions were considered: the total flume area and the ramp area:

$$A_T = H_T L_T \tag{1}$$

$$A_{r,i} = \frac{H_i L_i}{2} \tag{2}$$

where i = 1 and 2; H_T = 20*H and L_T = 5*λ.

The area fraction of the ramps is defined as:

$$\phi_i = \frac{A_{r,i}}{A_T} \tag{3}$$

It is intended with this study to maximize the available power (P_d) per meter of wavefront, thus the proposed equation is given by:

$$P_d = \frac{g h_{a,i,t_f}}{t_f} \int_{t_i}^{t_f} \dot{m}_i dt \tag{4}$$

where g is the gravitational acceleration (m/s^2), h_{a,i,t_f} is the water accumulation height inside the reservoir (m), t_i is the initial instant of time (s), t_f is the final instant of time (s) - in this case, t_f = 100 s - $\dot{m}$ is the mass flow rate of water entering into reservoir (kg/s).

Figure 3 shows the application of the Constructal Design in the geometric evaluation. Therefore, the fractions of area ϕ_1 and ϕ_2; and the ratio between the heights and lengths of the ramps H_1/L_1 and H_2/L_2 were kept fixed and given by the values 0.0006 and 0.3, respectively. However, for the distance between the ramps L_g, three values were adopted: 1.0 m, 1.5 m and 2.0 m; as well as for the height of the water depth h: 9.8 m, 10.0 m and 10.2 m; resulting in a total of nine simulations. Therefore, it is possible to define as restrictions of the problem: the total area of the flume, the ramp area, the lower ramp crown, the ramp slopes and the ramps area fractions. How degrees of freedom: the distance between the ramps and the depth of the water.

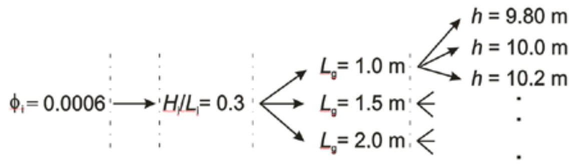

Figure 3. Illustration of the geometric evaluation process of the Constructal Design.

The Multiphase Volume of Fluid (VOF) Model

The Volume of Fluid method is used to evaluate the interaction of water with the device and, also, with the air. The VOF consists of a multiphase method which allows to study flows with two or more phases, particularly in this work the two phases (air and water) are immiscible (Hirt and Nichols, 1981).

The conservation equation of mass for the mixture of air and water in an isothermal, laminar and incompressible flow (Schlichting, 1979) is given by:

$$\frac{\partial \rho}{\partial t} + \nabla\left(\rho \vec{v}\right) = 0 \qquad (5)$$

where ρ is the density of the mixture (kg/m^3) and $\vec{v}$ is the flow velocity vector (m/s).

The momentum equation for the mixture is given by:

$$\frac{\partial \rho}{\partial t}\left(\rho \vec{v}\right) + \nabla\left(\rho \vec{v}\vec{v}\right) = -\nabla p + \nabla\left(\mu \bar{\bar{\tau}}\right) + \rho \vec{g} \qquad (6)$$

where p is the pressure (N/m²), $\rho\vec{g}$ is the buoyancy body force (N/ m³) and $\bar{\bar{\tau}}$ is the rate of deformation tensor (N/m²).

Was used for the air and water properties the following values: ρ_{air} = 1.225 kg/m³, ρ_{water} = 998.2 kg/m³, μ_{air} = 1.789×10^{-5} kg/(ms), μ_{water} = 1.003×10^{-3} kg/(ms).

Because two phases (air and water) are used in the study, the concept of volume fraction (α_q) is used to represent them within a control volume. In this model, the sum of the volume fractions must be unitary ($0 \leq \alpha_q \leq 1$). Therefore, when $\alpha_{water} = 0$, the control volume is empty of water and full of air ($\alpha_{air} = 1$), since when there is a mixture of air and water, one phase is the complement of the other, ie, $\alpha_{air} = 1 - \alpha_{water}$. Thus, an additional transport equation for the volume fractions is required (Hirt and Nichols, 1981):

$$\frac{\partial \alpha}{\partial t} + \nabla\left(\alpha \vec{v}\right) = 0 \qquad (7)$$

As the equation of conservation of mass and momentum are solved for the mixture, it is necessary to obtain density and viscosity values for the mixture, which can be written, respectively, by:

$$\rho = \alpha_{water}\rho_{water} + \alpha_{air}\rho_{air} \qquad (8)$$

$$\mu = \alpha_{water}\rho_{water} + \alpha_{air}\rho_{air} \qquad (9)$$

Regular Waves - Second Order Stokes Theory

For the present study, the Second Order Stokes Theory is adopted, because it is possible obtain a closer representation of the real waves even in the case of regular waves, thus allowing the analysis of higher waves at shallower depths. In this way, the velocity component *u* (horizontal direction x) and the velocity component *w* (vertical direction z) are given by (Chakrabarti, 2005):

$$u\left(x,z\right) = \frac{Hgk}{2\sigma}\frac{\cosh k(h+z)}{\cosh kh}\cos(kx-\sigma t) + \frac{3H^2\sigma k}{16}\frac{\cosh 2k(h+z)}{\sinh^4 kh}\cos 2(kx-\sigma t) \qquad (10)$$

$$w\left(x,z\right) = \frac{Hgk}{2\sigma}\frac{\sinh k(h+z)}{\cosh kh}\sin(kx-\sigma t) + \frac{3H^2\sigma k}{16}\frac{\sinh 2k(h+z)}{\sinh^4 kh}\sin 2(kx-\sigma t) \qquad (11)$$

where H is the wave height (m), g is the gravitational acceleration (m/s^2), k the wave number (m^{-1}), σ wave angular frequency (rad.s^{-1}), t time (s), h water depth (m), x horizontal coordinate, z vertical coordinate, u horizontal velocity (ms^{-1}) and w vertical velocity (ms^{-1}).

Boundary Conditions

As shown in Fig. 2, the numerical wave is generated on the lower left side (blue line - prescribed velocity) of the wave flume. The generation of the regular wave was given by the Second Order Stokes Theory, with the velocity components in the horizontal (x) and vertical (z) directions given by Equations (10) and (11).

In the upper left region, Fig. 2, and in the upper surface (green line) considered atmospheric pressure P_{abs} = 101.3 kPa. In the lower, right side surfaces and the surface of the overtopping device (red line) a non-slip condition and impermeability ($u = w = 0$ m/s) was imposed.

In relation to the initial conditions, it is considered that the fluid is flat, and the water depth h has the values: h = 9.8 m, 10.0 m and 10.2 m.

NUMERICAL PROCEDURES

The development of the study was done through the programs: for the preprocessing, creation of the geometry and the mesh, the commercial software Ansys Workbench 16® was used; for the processing, calculation of the partial differential equations (PDE), the commercial computational program Ansys Fluent 16®; and for post-processing the commercial spreadsheet editor Microsoft Excel 2010®.

The simulations were performed on a computer with a 3.3 Ghz Quad-Core AMD processor clock and 16 GB of RAM, and the Message Passing Interface (MPI) for parallelization. The processing time of each one of the simulations was approximately 7.92x10^4 s (~22 h).

Some of the parameters defined in the software Fluent 16® (based on Finite Volume Method (MVF), Patankar, 1980) were: pressure-based solver; first order advection scheme Upwind; Pressure Staggering Option (PRESTO) for the spatial discretization; the algorithm Pressure-Implicit with Splitting of Operators (PISO, Versteeg and Malalasekera, 2007) for pressure-velocity coupling; Geo-Reconstruction method for surface occupied by water; sub-relaxation factors of 0.3 and 0.7 for the conservation equations of mass and momentum. Furthermore, considered converged solution when the residual of the conservation equations of mass and momentum in the x and z directions were lower than 10^{-6}.

Figure 4 shows the refinement detail of the mesh, in which the Stretched mesh method was used with greater refinement in specific regions (Mavriplis, 1997). Therefore, the number of rectangular finite volumes of the meshes was close to 180,000.

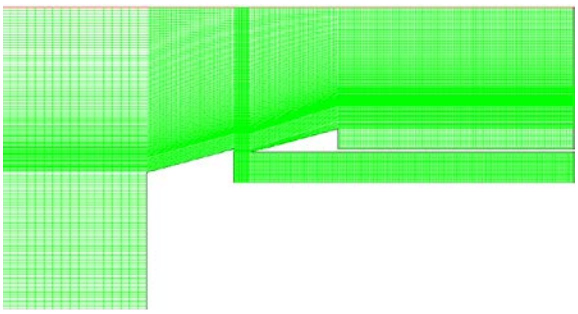

Figure 4. Illustration of the mesh used.

The present work adopted the theoretical recommendation proposed by Gomes et al. (2012) on the appropriate number of finite volumes for each region of the domain.

RESULTS AND DISCUSSION

Figure 5 shows the free surface elevation (η) obtained analytically and numerically for the Second Order Stokes Theory. To compare the significant maximum heights, the norm l_∞ is used (Kreyszig et al., 2011):

$$\|x\|_\infty = \max_j |x_j| \tag{12}$$

Thus, the value obtained for the analytical solution of the surface elevation was equal to 10.5233 m and for the numerical solution 10.6222 m, therefore the difference between the peaks is of 0.0998 m, acceptable value in face of the physical complexity of the problem, as presented in Gomes et al. (2016).

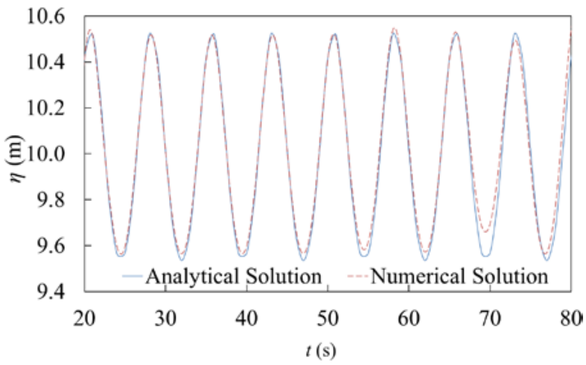

Figure 5. Comparison between analytical and numerical solutions by free surface elevation at position x = 50 m.

In Figure 6, the behavior of the available power (P_d) in relation to the distance between the ramps (L_g) and the water depth (h) for the lower ramp, can be analyzed. Therefore, when at low tide (depth h = 9.8 m) and for the three distances L_g (1.0, 1.5 and 2.0 m) P_d remained practically unchanged at the value of, approximately, 100 W/m.

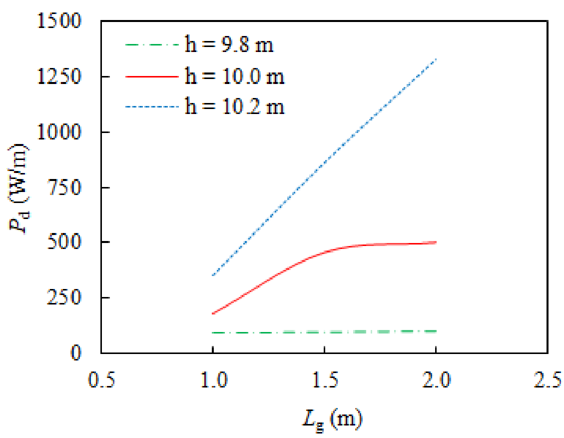

Figure 6. Influence of the parameter L_g and depth h on the available power (P_d) for the lower ramp.

For h = 10.0 m (mean depth considered) there was a increase of 2.5 times in P_d value (~180 to ~ 450 W/m) with an increase of L_g = 1.0 m for L_g = 1.5 m, and with the tendency to stabilize, from L_g = 2.0 m, in P_d ~450 W/m. However, for h = 10.2 m, the increase in P_d was expressive, from ~350 W/m to ~1330 W/m (~ 3.8 times), with an increase of L_g = 1.0 m for L_g = 2.0 m, and for L_g = 1.5 m the available power (P_d) was ~850 W/m.

The values presented are above relate to lower ramp, because for the upper ramp there was no significant accumulation of water.

Therefore, the shortest distances of L_g tends to complicate the accumulation of water in the lower reservoir of the ramp, as can be seen in the behavior of the available power (P_d), because of the water comes back to the flume. In addition, for the conditions proposed in this study, the optimal case must be determined for h = 10.0 m (average depth considered), the mean depth of sea level.

Thus, in this case the maximum available power ($(P_d)_m$) is equal to, approximately, 450 W/m to L_g = 2.0 m, because when a high tide (h = 10.2 m), P_d would be about 1330 W/m, compensating, the low power when low tide. In Figure 7 the same results are presented, however focusing on the influence of the depth variation h. Therefore, as expected, as the free water surface level increases, there is an increase in available power.

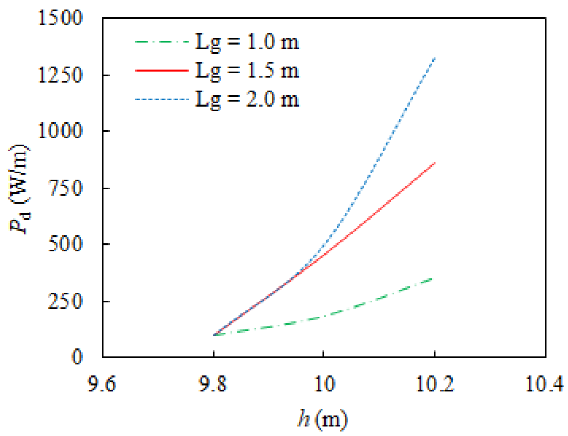

Figure 7. Influence of the depth h and the parameter L_g on the available power (P_d) for the lower ramp.

CONCLUSIONS

A numerical study was performed for the geometric evaluation of a real-scale coastal overtopping device with two ramps, varying the distance (L_g) between these and the water free surface (h - representing a tidal effect) with the purpose of evaluating the influence on the available power (P_d).

The ramp area fraction (ϕ_1 and ϕ_2) and the ramp height and length ratio (H_1/L_1 and H_2/L_2) were fixed, as well as the wave parameters: height (H) and period (T). In the geometric evaluation, the Constructal Design was used together with the Exhaustive Search optimization method. And the Second Order Stokes Theory for the reproduction of a regular sea wave.

The Constructal Design method has proved to be an important and interesting tool for the development of a geometric evaluation study, making it possible to establish a theoretical recommendation for engineering problems when in specific situations and conditions.

Therefore, the results indicated that the increase of the distance between the ramps (L_g), there was an increase in the available power (P_d). However, the water accumulation occurred exclusively on the lower ramp of the device. Furthermore, the influence of the tidal variations (represented by the three values of h) is significant, because when low tide (h = 9.8 m) the values of P_d were lower than those obtained at high tide (h = 10.2 m), as expected. Thus, the maximum available power ($(P_d)_m$) was considered for h = 10.0 m, mean sea level depth.

Thus, the high tide makes up for, in a way, the low tide period, since the value of P_d was approximately 13.3 times its value. However, further studies using other ramp configurations and sea conditions are required.

ACKNOWLEDGEMENTS

The Jaifer Corrêa Martins author thanks CAPES for the scholarship. The authors Luiz Alberto Oliveira Rocha, Liércio André Isoldi and Elizaldo Domingues dos Santos thank the CNPQ for their financial support.

REFERENCES

Almeida, L. E. S. B., Rosauro, N. M. L., and Toldo Jr., E. E., 1997, Análise Preliminar das Marés na Barra do Rio Tramandaí, RS, *in: Simpósio Brasileiro de Recursos Hídricos*, Vitória, ABRH, Vol. 1, pp. 7. (*in Portuguese*)

Ansys, 2016, *Theory Guide FLUENT 2016*.

Barbosa, D. V. E., Souza, J. A., Santos, E. D., Isoldi, L. A., and Martins, J. C., 2017, Numerical Analyses of Openfoam's Overtopping Device Solution, Revista Engenharia Térmica (Thermal Engineering), Vol. 16, pp. 96-103.

Bejan, A., and Lorente, S., 2008, *Design with Constructal Theory*, John Wiley & Sons.

Bejan, A., 2000, *Shape and Structure, From Engineering to Nature*, Cambridge University Press.

Chakrabarti, S. K., 2005, *Handbook of Offshore Engineering*, Elsevier.

Contestabile, P., Luppa, C., Di Lauro, E., Cavallaro, L., Andersen, L. T., and Vicinanza, D., 2017, Wave Loadings Acting on Innovative Rubble Mound Breakwater for Overtopping Wave Energy Conversion, Coastal Engineering, pp. 60-74.

Cruz, J. M. B. P., and Sarmento, A. J. N. A., 2004, *Energia das Ondas: Introdução aos Aspectos Tecnológicos, Econômicos e Ambientais*, Instituto do Ambiente, Alfragide. (*in Portuguese*)

Fleming, F. P., 2012, Avaliação do Potencial de Energias Oceânicas no Brasil, Master Thesis, COPPE-UFRJ, Rio de Janeiro, RJ. (*in Portuguese*)

Gomes, M. N., Costa, C. A. O., Deus, M. J., Ricardo, R. L. P., Isoldi, L. A., Santos, E. D., and Rocha, L. A. O., 2016, Análise Computacional e Geométrica com Design Construtal de um

Dispositivo Conversor de Energia das Ondas do Mar em Energia Elétrica do Tipo Coluna De Água Oscilante Submetido a um Espectro De Ondas, in: *Proceedings XXXVII Iberian Latin American Congresso on Computacional Methods in Engineering – CILAMCE 2016*, Brasília, Brasil. (*in Portuguese*)

Gomes, M. N., Santos, E. D., Isoldi, L. A., and Rocha, L. A. O., 2012, Análise de Malhas para Geração Numérica de Ondas em Tanques, in: *Proceedings VII Congresso Nacional de Engenharia Mecânica - CONEM 2012*, São Luiz, Brasil. (*in Portuguese*)

Goulart, M. M., Martins, J. C., Junior, I. C. A., Gomes, M. das N., Souza, J. A., Rocha, L. A. O., Isoldi, L. A., and Santos, E. D., 2015, Constructal Design of an Onshore Overtopping Device in Real Scale for Two Different Depths, Marine Systems & Ocean Technology, Vol. 10, pp. 1-10.

Hirt, C. W., and Nichols, B. D., 1981, Volume of Fluid (VOF) Method for the Dynamics of Free Boundaries, Journal of Computational Physics, Vol. 39, pp. 201-225.

Jungrungruengtaworn, S., and Hyun, B. S., 2017, Influence of Slot width on the Performance of Multi-Stage Overtopping Wave Energy Converters, International Journal of Naval Architecture and Ocean Engineering, Vol. 9, pp.1-9

Kreyszig, E., Kreyszig, H., and Norminton, E. J., 2011, *Advanced Engineering Mathematics*, 10th Edition, John Wiley & Sons.

Lisboa, R. C., Teixeira, P. R. F., and Didier, E., 2016, Simulação de Propagação de Ondas Regulares e Irregulares em um Canal Bidimensional com Praia Numérica, in: *VII Seminário e Workshop em Engenharia Oceânica*, Rio Grande. (*in Portuguese*)

Liu, Z., Shi, H., Cui, Y., and Kim, K., 2017, Experimental Study on Overtopping Performance of a Circular Ramp Wave Energy Converter, Renewable Energy, Vol. 104, pp.163-176.

Machado, B. N., Dos Santos, E. D., Isoldi, L. A., Gomes, M. N., and Rocha, L. A. O., 2017, Análise Numérica da Geometria da Rampa de um Dispositivo de Galgamento Onshore em Escala Real Aplicando o Design Construtal, Revista Brasileira de Energia Renováveis, Vol. 6, pp. 548-566. (*in Portuguese*)

Margheritini, L., Stratigaki, V., and Troch, P., 2012, Geometry Optimization of an Overtopping Wave Energy Device Implemented into the New Breakwater of the Hanstholm Port Expansion, in: *Twenty-second International Offshore and Polar Engineering Conference*, pp. 593-600.

Margheritini, L., Vicinanza, D., and Frigaard, P., 2009, SSG Wave Energy Converter: Design, Reliability and Hydraulic Performance of an Innovative Overtopping Device, Renewable Energy, Vol. 34, pp.1371-1380.

Martins, J. C., Goulart, M. M., Souza, J. A., Isoldi, L. A., Dos Santos, E. D., Gomes, M. N., and Rocha, L. A. O., 2015, Constructal Design of an Onshore Overtopping Device in Real Scale for Different Ramp Construction Areas, in: *23rd ABCM International Congress of Mechanical Engineering*, Rio de Janeiro, RJ, Vol. 1.

Martins, J. C., Goulart, M. M., Gomes, M. N., Souza, J. A., Rocha, L. A. O., Isoldi, L. A., and Dos Santos, E. D., 2017, Análise Numérica de um Dispositivo de Galgamento Onshore Comparando a Influência de uma Onda Monocromática e de um Espectro de Ondas, Revista Brasileira de Energia Renováveis, Vol. 6, pp. 472-488. (*in Portuguese*)

Martins, J. C., Goulart, M. M., Gomes, M. N., Souza, J. A., Rocha, L. A. O., Isoldi, L. A., and Dos Santos, E. D., 2018, Geometric Evaluation of the Main Operational Principle of an Overtopping Wave Energy Converter by Means of Constructal Design, Renewable Energy, Vol. 118, pp. 727-741.

Mavriplis, D. J., 1997, Unstructured Grid Techniques, Annual Reviews Fluid Mechanics, Vol. 29, pp. 473-514.

Nørgaard, J. H., and Andersen, T. L., 2012, Investigation of Wave Transmission from a Floating Wave Dragon, in: *Proceedings of the Twenty – Second (2012) International Offshore and Polar Engineering Conference*, Rhodes, Greece, Vol. 22, pp. 509-516.

Patankar, S. V., 1980, *Numerical Heat Transfer and Fluid Flow*, McGraw Hill.

Schlichting, H., 1979, *Boundary Layer Theory*, 7th Edition, McGraw-Hill.

Versteeg, H. K., and Malalasekera, W., 2007, *An Introduction to Computational Fluid Dynamics: The Finite Volume Method*, Pearson.

Vicinanza, D., Cantestabile, P., Nørgaard, J. Q. H., and Andersen, T. L., 2014, Innovative Rubble Mound Breakwaters for Overtopping Wave Energy Conversion, Coastal Engineering, Vol. 88, pp. 154-170.